Basal Melt Beneath Whillans Ice Stream and Ice Streams A and C

Ian R. Joughin
Jet Propulsion Lab
M/S 300-235
4800 Oak Grove Drive
Pasadena, CA 91109, United States
818-354-1587 (voice)
818-393-3077 (fax)
ian@radar-sci.jpl.nasa.gov

Slawek Tulaczyk
University of California, Santa Cruz
A208 Earth and Marine Sciences Bldg.
Santa Cruz, CA 95064, United States
831-459-5207 (voice)
831-459-3074 (fax)
tulaczyk@es.ucsc.edu

Hermann Engelhardt
208 N. Mudd
M/C 100-23
Pasadena, CA 91125
(626) 395-3720 (voice)
engel@caltech.edu

We have used a recently derived map of the velocity of Whillans Ice Stream and Ice Streams A and C to help estimate basal melt. Temperature was modeled with a simple vertical advection-diffusion equation, "tuned" to match temperature profiles. We find that most of the melt occurs beneath the tributaries where larger basal shear stresses and thicker ice favors greater melt (e.g., 10-20 mm/yr). The occurrence of basal freezing is predicted beneath much of the ice plains of Ice Stream C and Whillans Ice Stream. Modelled melt rates for when Ice Stream C was active suggest there was just enough melt water generated in its tributaries to balance basal freezing on its ice plain. Net basal melt for Whillans Ice Stream is positive due to smaller basal temperature gradients. Modelled temperatures on Whillans Ice Stream, however, were constrained by a single temperature profile at UpB. Basal temperature gradients for Whillans B1 and Ice Stream A may have conditions more similar to those beneath Ice Streams C and D, in which case, there may not be sufficient melt to sustain motion. This would be consistent with the steady deceleration of Whillans stream over the last few decades.

Topics Ice Streams (3) and Basal boundary conditions (4).

Introduction

Fast motion of Whillans Ice Stream is enabled by a several-meter thick layer of water-saturated dilatant till [Blankenship and others 1987; Alley and others 1987]. Similar basal conditions are likely responsible for the fast motion of Ice Stream C when it was active [Atre and Bentley,1993]. Whether a viscous deforming till [Alley and others, 1987; Kamb 2001] or a weak plastic bed [Kamb, 1991; Tulaczyk and others, 2000ab] is responsible for the motion, water is an essential ingredient for the fast flow of these ice streams.

Early estimates predicted high (~20 mm/yr) basal melt beneath the Ross Ice Streams [Rose, 1979; Shabtaie and Bentley, 1987]. Since then several studies [Whillans and others, 2001] have shown that ice stream shear margins can support much of the driving stress and there is significantly less basal shear heating with which to melt ice [Raymond, 2000]. Studies investigating the heat balance of ice stream have found that, at least in some well lubricated areas, it is difficult to sustain basal melting [Hulbe, 1998; Raymond, 2000]. Other studies have suggested that the ice stream catchments provide sufficient melt water to sustain motion [Parizek and Alley, 2001].

Ice stream C stopped about 150 years ago [Retzlaff and Bentley, 1993] and Whillans Ice Stream has undergone substantial deceleration over the last few decades [Whillans and others 2001, Joughin and others, in press]. This deceleration has caused Whillans Ice Stream to go from having a significantly negative mass balance to the point where it is presently close to balance [Joughin and Tulaczyk, 2002]. Extrapolation of the recent deceleration rates suggests the ice stream could stop within 70-80 years. Understanding the shutdown of Ice Stream C and the future behavior of Whillans Ice Stream depends on improving our knowledge of basal melt/freeze conditions beneath these ice streams.

Recent advances in interferometric synthetic aperture radar (InSAR) have allowed nearly a complete mapping of the Ross Ice Streams and their tributaries [Joughin and others, in press]. These data have revealed an extensive network of tributaries feeding the ice streams [Joughin and others, 1999]. With thicker ice and significantly higher basal shear stresses than beneath the ice streams [Joughin and others, in press], significantly more melting should occur beneath the tributaries than their respective ice streams. The remainder of this paper describes estimates of basal melt we derived using both the velocity and borehole temperature data.

Melt Rate Estimation and Assumptions

We estimated basal melt rate, m_r, using [Paterson, 1994]

$$m_r = \frac{G + \tau_b U_b - k_i \Theta_b}{L_i \rho_{ice}}, \tag{1}$$

where G is the geothermal heat flux, τ_b is the basal shear stress, U_b is basal speed, k_i is the thermal conductivity for ice, Θ_b is the basal temperature gradient, L_i is the latent heat of fusion, and ρ_{ice} is the density of ice. The difficulty in applying this equation is in obtaining estimates of G, Θ_b, and basal shear heating, $\tau_b U_b$. The remainder of this section describes the assumptions we used in deriving melt rate estimates.

Geothermal Heat Flux

We used a value of G=70 mW/m^2, which is the value that was determined from a borehole at Siple Dome [HERMANN REF]. This measurement of geothermal heat flux is the closest in location to our study area and we have used this value in all our estimates. The sensitivity of our estimates to geothermal heat flux is easily evaluated since a change in G by 10 mW/m^2 changes m_r by about 1 mm/yr.

Basal Temperature Gradient

The basal temperature gradient can be calculated easily if the temperature profile within the ice column is known. There are only a few measured temperature profiles, however, so we are forced to use a model to estimate Θ_b. If we assume only vertical thermal diffusion and advection with a bed temperature at the pressure melting point, T_{pmp}, an analytical steady state solution [Zotikov, 1986, Equation 4.17] for temperature as a function of depth is given by,

$$T = T_{pmp} + (T_S - T_{pmp}) \frac{\mathrm{erf}\left(\sqrt{0.5Pe}\frac{z}{H}\right)}{\mathrm{erf}(\sqrt{0.5Pe})}, \quad (2)$$

where, T_S is the surface temperature, H is ice thickness, and z denotes the vertical coordinate (zero at the bed and H at the top). The Peclet number is defined as $Pe = \frac{aH}{\kappa}$, where a is the surface accumulation rate and κ is the thermal diffusivity of ice.

Temperature profiles have been measured on ice streams at the UpB [Engelhardt and Kamb, 1993], UpC [XXX], and UpD [XXX] camps. Additional profiles not on ice streams have been measured at Byrd Station [Gow and others, 1968], the Unicorn (the ridge separating Whillans Branch 1 (B1) and Whillans Branch 2 (B2)) [Engelhardt and Kamb, 1993], and at Siple Dome [HERMANN REF]. We used these measurements to examine the validity Equation (2) for estimating the basal temperature gradient.

We used gridded accumulation data, a_{Giov} [Giovinetto *et al.*, 1990; Giovinetto and Bentley, 1985] to estimate temperature using Equation (2). For ice thicknesses, we used the BEDMAP data set [Lythe and others, 2001]. The Unicorn and Siple Dome profiles have frozen beds so that Equation (2) does not apply. Closed form solutions exist for this case, but we instead used an equivalent simple numerical model to solve the heat balance equation with vertical advection and diffusion

for a frozen bed.

Table 1 shows a comparison of the modeled and measured temperature profiles. The Root Mean Squared (RMS) difference (Table 1, column 4) between the measured and modelled profiles exceeds 3^{o} in some cases. Plots of the modeled (green) and measured (red *) temperature profiles at the UpC and UpB camps are shown in Figure 1. At UpC in particular, the model provides a poor representation of the actual temperature profile, with the model underestimating the basal temperature gradient by 40% (Table 1, column 6).

If we assume the ice stream geometry and thermal diffusivity are fixed, then the only free parameter in equation (2) is the accumulation rate. We adjusted this parameter to obtain an "effective" accumulation rate, a_{eff}, that minimizes the model-data misfit [Joughin and others, in press]. The results of this experiment are summarized in Table 1 and indicate that the model-data misfit can be reduced below 1^{o} and in many cases to within a few tenths of a degree. The blue curves in Figure 1 show the improved agreement using a_{eff} at the UpB and UpC camps.

The value of a_{eff} is more than three times a_{Giov} for the UpC, UpD, and Unicorn profiles. At Siple Dome, where conditions are likely the most consistent with the model assumptions, there is only a small difference between a_{eff} and a_{Giov}. This means it is unlikely that past changes in accumulation or temperature can explain the cases where the differences are large, since the climate history should similar at all the borehole sites. Instead, since the UpD and UpC camps are fed by relatively fast flowing (50-100 m/yr) tributaries that originate near the ice divide, rapid horizontal advection of cold ice from the interior may explain the difference [Joughin and others, in press].

While the a_{eff} value improves the fit at UpB, the difference relative to a_{Giov} is not nearly as large as for UpC and UpD cases. This may be because the UpB area is fed by relatively slow-moving

ice drawn from not far upstream so that the temperature profile is more strongly influenced by the local accumulation rate and temperature [Joughin and others, in press]. It is interesting then that the greatest difference between a_{eff} and a_{Giov} occurs at the Unicorn borehole, which is located not far from the UpB camp (see Figure 2). This difference is especially interesting, considering that the other two boreholes located in slow moving ice (Siple Dome, Byrd) show relatively little disparity between a_{eff} and a_{Giov}. Recent analysis of ice penetrating radar data, however, suggests that the ice near the Unicorn borehole was part of Whillans B2 ~190 years ago [Clarke and others, 2000]. Examination of the velocity map [Joughin and others, in press] indicates that the flow in this region may originate from a ice stream tributary that is distinct from the origin of flow at the UpB camp. This tributary extends significantly farther inland to near the Transantarctic Mountains and passes through a strong gradient in surface temperature [Fahnestock and Bamber, 2001]. Ice Stream A and Whillans B2 are also fed from tributaries that extend deep inland. Consequently, the basal temperature gradients on much of the ice plain of Whillans Ice Stream could more closely resemble those at UpC and UpD than those at UpB.

We computed melt rate estimates for Ice Stream C and Ice Stream A/Whillans Ice Stream separately using a fixed accumulation rate for each basin (see basin division Figure 2). The data in Figure 1 indicate we should obtain a better estimate of Θ_b using a_{eff} in Equation (2) in rather than the actual accumulation rates, at least in the fast flow regions in the vicinity of the boreholes. The data at Byrd Station suggest we would obtain a better estimate of the basal temperature gradient with a_{Giov}. This borehole, however, is located on a slower moving area where there is likely to be little horizontal advection. In the experiments described below we varied the accumulation rate to determine its impact on melt.

Basal Shear Heating

Basal velocity, U_b, and shear stress, τ_b, are needed to determine basal shear heating in Equation (1). We have measured surface velocities [Joughin and others, 2001] over much of the study area. These data provide a good approximation of the basal velocity, since in most cases there is little vertical shear within the ice column. There are a few gaps in the velocity map that we crudely filled with a constant similar to that of the surrounding values.

We also generated a rough estimate of the balance velocity for Ice Stream C when it was active. First, we estimated the constant balance velocity across a profile near the grounding line for estimated flux of ice through the profile of 22.5 km^3/yr (Joughin and Tulaczyk, 2002). This yielded a balance velocity estimate of 387 m/yr, which is similar to the speed of the other Ross ice streams. Next, we took advantage of the fact that there is relatively little variation in the width of the formerly active area of Ice Stream C. This allowed us to compute a very rough estimate of the balance velocity as the product of the gate thickness and balance velocity divided by the thickness at each point. Figure 2 shows velocity contours for the resulting estimate. Our goal here was limited to obtaining representative velocities for use in equation (1) and was not to reconstruct in detail the former flow field of Ice Stream C.

Force balance estimates that indicate that basal shear stress in the ice stream tributaries resists ~50% of the driving stress [Joughin and others in press]. Based on this observation and to simplify the model, we assumed that $\tau_b=0.5\tau_d$ for the tributaries. An exception was the large tributary flowing through the Bentley subglacial trough where force balance estimates suggest a factor of 0.85 should be used. On the currently active part of Ice Stream C, force balance estimates indicate a value of $\tau_{b,active}$ = 11.6 kPa [Joughin and others, in press]. This value was likely smaller when

the ice stream was fully active, suggesting less basal shear heating at that time. On the other hand, speeds were likely greater when the ice stream was active, which would increase basal shear heating. Lacking more detailed knowledge of conditions at the time of stagnation, we used the current values of velocity and τ_b for the still active portion of the ice stream.

On the fast flowing parts (U_b > 150 m/yr) of the ice streams we assumed a constant value of τ_b. In most experiments we used τ_b=2 kPa, which is consistent with force balance estimates [Whillans and van der Veen, 1997] and laboratory measurements [Tulaczyk, 2000a]. In the model and in the discussion below, 150 m/yr is used as a somewhat arbitrary threshold to distinguish between ice stream and tributary flow.

Regions with Basal Melt

Equation (2) applies only to the case where the bed is melted. We made the assumption in our estimates that the bed was melted where flow speed was greater than 25 m/yr. For all slower moving areas, we assumed the bed was frozen with zero melt. This is a good approximation for the catchments of Ice Stream A and Whillans Ice Stream. Some of the deep inland ice in the upper catchment of Ice Stream C could experience some basal melt in regions with speeds of less than 25 m/yr. We estimate, however, that the basal melt in this region is less than 10% of the melt generated in the tributaries feeding Ice Stream C.

The black lines in Figure 2 show present day estimates of the catchments divides for each ice stream (Joughin and Tulaczyk, 2002). The divide estimates indicate that Whillans B2 has captured some of the drainage from Ice Stream C when it was active. Since we are interested in conditions when Ice Stream C was active, we have decided to separate melt water production in the Ice Stream C and Whillans Ice Stream catchments as shown by the white line in Figure 2. This is a

rough approximation of the former divide and it was designed only to separate melt estimates in tributaries that used to feed Ice Stream C from those that fed Whillans Ice Stream.

Model Results

We computed melt rates using Equation (1) and the assumptions described above. The results for Ice Stream A/Whillans Ice Stream are summarized in Table 2 and the results for Ice Stream C are summarized in Table 3. In each case, we ran an initial experiment (W1, C1) based on our best estimate of the parameters needed to determine melt rate. There is a reasonable amount of uncertainty in these parameters, so we conducted several additional experiments (W2-W6, C2-C8) to examine the sensitivity of melt rate estimates to the model parameters.

Our initial experiment (W1) for Ice Stream A and Whillans Ice Stream yielded a net melt rate of 1.9 mm/yr with a 4.8-mm/yr net melt rate for the tributaries and a net freeze-on rate of 1.1 mm/yr for the ice streams. The spatial pattern of melt for this experiment is shown in Figure 2. Whillans B1 and B2 are estimated to have only slightly positive melt rates, while on much of the ice plain basal freeze-on is estimated to occur at rates of 1-2 mm/yr. There is a region near Crary Ice Rise with freeze-on rates of about 6 mm/yr. In experiment W2, we used a= 0.295 m/yr, which yielded a net basal freeze-on rate of 1.0 mm/yr. Experiments W3-W5 demonstrate the sensitivity of melt to basal shear stress. We note that the value of τ_b=5 kPa in experiment W5 is unrealistically high for much of the ice plain since it exceeds the driving stress in some places. In experiment W6 we evaluated the change a decrease in total melt rate to 1.2 m/yr in response to a 100-m thinning of the ice sheet with sufficient time to reach a new steady-state temperature profile.

We conducted a similar set of experiments for Ice Stream C (C1-C8). In C1 we used a_{eff}= 0.295 m/yr, which is the value derived from the borehole temperature fits. With this value, the ice stream

would have had an average melt rate of only 0.3 mm/yr when it was active. Figure 2 indicates that the freeze-on rates on the active Ice Stream C likely ranged from about 4 to 8 mm/yr. If instead we use the effective accumulation rate for Whillans Ice Stream (a_{eff}=0.16 m/yr), then the total average melt rate increases to 3.1 mm/yr in experiment W2. In varying the basal shear stress (C2-C5) the range of average melt rates varies from 0.0 to 2.1 mm/yr. Thinning the ice stream by 100 m yields a net freeze-on rate of 0.1 mm/yr. In experiment C7, we reduced the velocity on the formerly active portion of Ice Stream C to close to its present day value. This increased the basal freeze-on rate on the ice stream from 5.7 to 7.1 mm/yr. In experiment C8, we increased the active ice stream velocity estimate by 50%, which increased the total melt rate by 0.4 mm/yr.

Discussion

Even with considerable variation of the model parameters, our results indicate that, by in large, melting takes place beneath ice stream tributaries, while low-melt or freeze-on conditions prevail beneath the active parts of Whillans Ice Stream and Ice Stream C. Unless we increase τ_b to unrealistically high levels, the model consistently predicts basal freezing beneath the thin ice of the ice plains. This indicates that, as suggested earlier by Raymond [2000], import of basal melt from upstream appears to be a necessary condition to sustain motion on these ice streams. It is not a sufficient condition, however, since an appropriate drainage network is also required to redistribute the water from melting to freezing regions.

If ice stream tributaries by virtue of their higher-basal shear stress and thicker ice are the primary source of water that enables fast ice stream flow, then this raises the issue of what length ice streams they could support. If grounding lines of Ice Stream C and Whillans Ice Stream were extended seaward by 10's of km with similar thickness to their respective ice plains, then the area

with net basal freeze-on would eventually outcompete the area with net basal melt. The distance from the meltwater source would also increase, placing additional constraints on the drainage network. Thus, it is likely that some additional basal melt source beyond that of the present day tributaries is necessary to sustain very long paleo ice streams. Multibeam sonar data indicate there were likely regions of exposed bed rock beneath portions of the Ross paleo ice streams [Anderson and Shipp, 2000], which perhaps could have provided basal shear heating to enable additional melt.

Flow speed on Whillans Ice Stream has decreased significantly over the last few decades [Whillans and others, 2001; Joughin and others, in press]. Experiment W1 suggests that presently there may be sufficient melt to sustain motion, with possible additional melt water from diversion of water from Ice Stream C [Alley and others, 1994]. The Unicorn temperature data, however, suggest that the temperature gradients for Whillans B1 and Ice Stream A may be closer to those of Ice Stream C than of Whillans B2. In this case, experiment W2 may better represent conditions beneath the ice stream. If this is so, then Whillans Ice Stream may well be headed toward complete stagnation within this century as the recent deceleration rates suggest. These results argue strongly in favour of additional drilling on the ice plain of Whillans Ice Stream to better constrain temperature estimates there.

The results for Ice Stream C yield average melt rates near zero. This means that the motion of the ice stream was particularly sensitive to piracy of basal melt water [Alley, 1994]. In our experiments, we have assigned all the melt from the tributary that now appears to have been diverted to the catchment of Whillans B2 (see flow divides in Figure 2). Diversion of the basal water flow from this tributary alone would likely have been sufficient to initiate stagnation. On the other

hand, conditions may have been so close to zero net melt (experiment C1) that stagnation could also have occurred without resorting to water piracy [Price and others, 2001; Bougamont and others, submitted].

Our experiments reveal a strong sensitivity to accumulation rate when only vertical advection and diffusion are considered in estimating melt rate. Our attempts to use an effective accumulation rate correct some of the deficiencies in the model, resulting in better melt rate estimates. This is clearly an artificial effect that compensates for inadequacies in the model and does not suggest change in accumulation rate. While it appears that temperature estimates are improved, it is not very satisfying in that it does not explain the inadequacies of the model. We hypothesize that the model fails because tributary flow is strong enough to significantly depress basal melting through strong horizontal advection of ice from the interior. More detailed flowline and 3-D ice flow modeling along with more borehole temperature data are required to test this hypothesis.

Acknowledgements

I. Joughin performed his contribution to this work at the Jet Propulsion Laboratory, California Institute of Technology, under contract with NASA. S. Tulaczyk was funded under by the National Science Foundation (NSF-OPP-0096302). The RADARSAT data were acquired by the Canadian Space Agency and were downlinked and processed to L0-products by the Alaska SAR Facility. Mosaicked RADARSAT images and the surface DEM were provided by K. Jezek of the Byrd Polar Research Center. D.G. Vaughan and the BEDMAP project produced the bed topography DEM. Many of the data sets we used were archived at the National Snow and Ice Data Center.

References

Alley R.B., D.D. Blankenship, C.R. Bentley, S.T. Rooney. 1987. Till beneath Ice Stream-B. 3. Till deformation - evidence and implications, *J. Geophys. Res.*, **92**(B9), 8921-8929.

Alley, R.B., S. Anandakrishnan, C.R. Bentley, and N. Lord. 1994. A water piracy hypothesis for the stagnation of Ice Stream C, Antarctica, *Ann. of Glaciol.*, **20**, 187-194.

Anderson, J.B. and S.S. Shipp. 2001. Evolution of the West Antarctic Ice Sheet, AGU *Antarctic Research Series*, 77, 45-57.

Atre S.R., and C.R Bentley. 1993. Laterally varying basal conditions beneath Ice Stream-B and Ice Stream-C West Antarctica. *J. Glaciol.*, **39**(133) 507-514.

Blankenship D.B., C.R. Bentley, S.T. Rooney, R.B. Alley. 1987. Till beneath Ice Stream-B. 1. Properties Derived from seismic travel-times," *J. Geophys. Res.*, **92**(B9), 8903-8911.

Bougamont, M., S. Tulaczyk, and I. Joughin. Submitted. Response of subglacial sediments to basal freeze-on: II. Application to the stoppage of Ice Stream C, West Antarctica, to be submitted to *J. Geophys. Res.*, March 2002.

Clarke T.S., L. Chen, N.E. Lord, and C.R. Bentley. 2000. Evidence of a recently abandoned shear margin adjacent to ice stream B2, Antarctica, from ice-penetrating radar measurements. *J. Geophys. Res.*, **105**(B6) 13,409-13,422.

Hamilton, G.S. In press. Mass balance and accumulation rate across Siple Dome, West Antarctica. *Ann. Glaciol.*

Engelhardt, H., and B. Kamb. 1993. Vertical temperature profile of Ice Stream B, Antarctica. *Antarctic J. U.S.*, **28**(5), 63-66.

Fahnestock M. and J. Bamber, 2001. "Morphology and surface characteristics of the West Antarctic ice sheet, AGU *Antarctic Research Series*, 77, 13-27.

Gow, A.J., H.T. Ueda, and D.E. Garfield. 1968. Antarctica ice sheet: preliminary results of the first core hole to bedrock. *Science*, **161**, 1011-1013.

Hulbe, C.L. 1998. Heat balance of West Antarctic ice streams, investigated with numerical models of coupled ice sheet, ice stream, and ice shelf flow. (Ph.D. thesis, University of Chicago).

Joughin, I., and S. Tulaczyk. 2002. Positive mass balance of the Ross Ice Streams, West Antarctica, *Science*, 295, 476-480.

Joughin, I., L. Gray, R. Bindschadler, S. Price, D. Morse, C. Hulbe, K. Mattar, and C. Werner. 1999. Tributaries of West Antarctic ice streams revealed by RADARSAT interferometry, *Science*, 286, 283-286.

Joughin I., S. Tulaczyk, R. Bindschadler, S.F. Price. In press. Changes in West Antarctic Ice Stream Velocities: Observation and Analysis, *J. Geophys. Res. Solid Earth.*

Lythe, M.B., D.G. Vaughan, and the BEDMAP Consortium. 2001. BEDMAP: A new ice thickness and subglacial topographic model of Antarctica, *J. Geophys. Res.*, 106(B6), 11335-11351,.

Kamb, B., Basal zone of the West Antarctic Ice Streams and its role in lubrication of their rapid motion, AGU *Antarctic Research Series*, 77, 157-200, 2001.

Kamb, B., 1991, Rheological nonlinearity and flow instability in the deforming-bed mechanism of ice stream motion, *J. Geophys. Res.*, 96(B10), 16,585-16,595, 1991.

Parizek B.R. and R.B. Alley. 2001. Cumulative melt beneath the ice-stream catchments: A source of long-term stability for the Siple Coast ice streams? Present at the *2001 WAIS Workshop,* Sterling, VA.

Price, S.F., R.A. Bindschadler, C.L. Hulbe, and I.R. Joughin. 2000. Post-stagnation behavior in the upstream regions of Ice Stream C, West Antarctica, *J. Glaciol.* **47**(157), 283-294.

Raymond, C.F. 2000. Energy balance of ice streams, *J. Glaciol.* **46**(155), 665-674.

Retzlaff, R., and C.R. Bentley. 1993. Timing of stagnation of Ice Stream C, West Antarctica, from short-pulse radar studies of buried surface crevasses, *J. Glaciol.* **39**(133), 552-561.

Rose, K.E., 1979. Characteristics of ice flow in Marie Byrd Land, Antarctica, *J. Glaciol.*, **24**(90), 63-75.

Shabtaie S. and C.R. Bentley. 1987. West Antarctic Ice Streams draining into the Ross Ice Shelf - Configuration and mass balance, *J. Geophys. Res.*, **92**(B2), 1311-1336.

Tulaczyk, S., W.B. Kamb, and H.F. Engelhardt. 2000a. Basal mechanics of Ice Stream B, West Antarctica 1. Till mechanics, *J. Geophys. Res.*, 105(B1), 463-481.

Tulaczyk, S., Kamb W.B., and H.F. Engelhardt. 2000b. Basal mechanics of Ice Stream B, West Antarctica 2. Undrained plastic bed model, *J. Geophys. Res.*, 105(B1), 483-494.

Whillans, I.M., C.R. Bentley, and C.J. Van der Veen. 2001. Ice Streams B and C, AGU *Antarctic Research Series*, 77, 257-282.

Whillans, I.M., and C.J. Van der Veen, 1997. The role of lateral drag in the dynamics of ice stream B, Antarctica, *J. Glaciol.* **43**(144), 231-237.

Table 1: Comparison of modelled and measured temperature profiles at the borehole locations shown in Figure 2.

Location	a_{Giov} mm/yr of ice	a_{eff} mm/yr of ice	RMS misfit for a_{Giov} (°C)	RMS misfit for a_{eff} (°C)	Θ_b for a_{Giov} (°C/m)	Θ_b for a_{eff} (°C/m)	Θ_b measured (°C/m)
UpB	0.106	16.0	1.25	0.15	0.035	0.041	0.045
UpC	0.100	29.5	3.33	0.72	0.033	0.053	0.054
UpD	0.101	33.0	2.75	0.27	0.032	0.053	0.052
Siple Dome[a]	0.133[b]	10.0	0.73	0.28	0.037	0.033	0.036
Unicorn[a]	0.106	42.0	3.74	0.41	0.032	0.058	0.051
Byrd	0.16	22.0	1.4	0.78	0.030	0.035	0.029

a. Numerical model with vertical advection and diffusion used with surface and basal temperature boundary conditions from profile.
b. From a single core measurement [Hamilton, in press].

Table 2: Model results for several experiments on Whillans Ice Stream and Ice Stream A.

Experiment	Experiment Parameters	m_{trib} mm/yr	m_{icest} mm/yr	m_{tot} mm/yr
W1	$\tau_{b,\,icest}$ = 2 kPa, $\tau_{b,\,trib}$ = 0.5τ_d, a=0.16 m/yr	4.8	-1.1	1.9
W2	Same as 1 but with a=0.295 m/yr	1.9	-4.1	-1.0
W3	Same as 1 but $\tau_{b,\,trib} = \tau_d$	11.9	-1.1	5.6
W4	Same as 1 but $\tau_{b,\,icest}$ = 1 kPa,	4.8	-2.3	1.4
W5	Same as 1 but $\tau_{b,\,icest}$ = 5 kPa,	4.6	2.3	3.6
W6	Same as 1 but ice thinned by 100 m	4.4	-2.1	1.2

Table 3: Model results for several experiments on Ice Stream C.

Experiment	Experiment Parameters	m_{trib}	m_{icest}	m_{tot}
C1	$\tau_{b,\,icest} = 2\,\text{kPa}$, $\tau_{b,\,trib} = 0.5\tau_d$, $\tau_{b,\,Bentley} = 0.8\tau_d$, $\tau_{b,\,active} = 11.6\,kPa$, a=0.295 m/yr	2.8	-4.9	0.3
C2	Same as C1 but with a=0.16 m/yr	5.4	-1.8	3.1
C3	Same as C1 but $\tau_{b,\,trib} = \tau_d$, $\tau_{b,\,Bentley} = \tau_d$	5.4	-4.9	2.1
C4	Same as C1 but $\tau_{b,\,icest} = 1\,\text{kPa}$,	2.8	-6.0	0.0
C5	Same as C1 but $\tau_{b,\,icest} = 5\,\text{kPa}$,	2.8	-1.4	1.4
C6	Same as C1 but ice thinned by 100 m	2.5	-5.7	-0.1
C7	Same as C1 but with ~10 m/yr velocity on stagnant region	2.8	-7.1	-0.4
C8	Same as 1 but with a 50% increase over balance velocity estimate.	2.8	-3.7	0.7

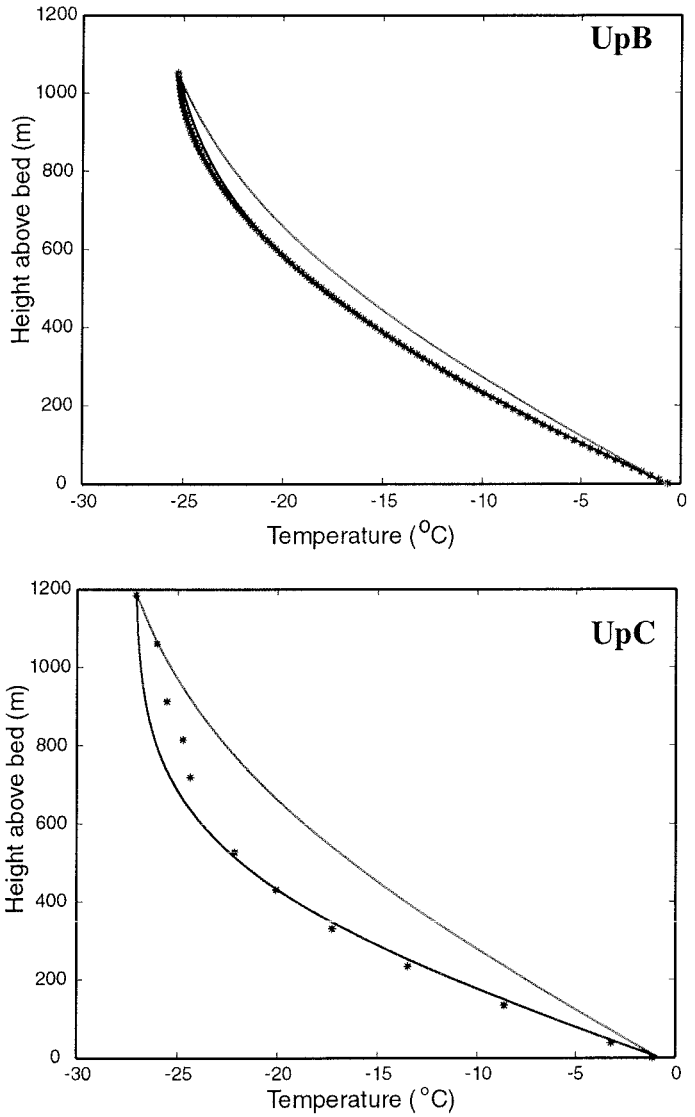

Figure 1. Modelled (solid lines) and measured (red *) temperature profiles at the UpB and UpC camps. The green lines show the model result using the measured accumulation. The blue curves are for the "effective" accumulation rate that minimizes the model/data misfit.

Figure 2. Estimated melt rate for Ice Streams A and C and Whillans Ice Stream for experiments W1 and C1 (see Table 2 and Table 3). Thick black lines show ice stream catchment divides for present day geometry (Joughin and Tulaczyk, 2002). White line shows division of basal melt between ice stream C and Whillans Ice Stream that was used for estimating the individual ice stream estimates given in Table 2 and Table 3. Thin black lines flow speed contours at intervals of 50 m/yr. High freeze-on rates in the upper parts of Ice Stream A and Whillans Ice Stream likely reflects erroneously thin ice where sparse thickness data do not fully resolve thick ice in narrow subglacial valleys. The color bar saturates at +20 mm/yr, so higher melt rates are possible in limited areas.